Inorg. Chem. **2005**, *44*, 5903–5910

Synthesis, Structure, and Magnetism of Heterometallic Carboxylate Complexes $[Mn^{III}_2M^{II}_4O_2(PhCOO)_{10}(DMF)_4]$, M = Mn^{II}, Co^{II}, Ni^{II}

Konstantin S. Gavrilenko,[†,‡] Sergey V. Punin,[‡] Olivier Cador,[†] Stéphane Golhen,[†] Lahcène Ouahab,*[,†] and Vitaly V. Pavlishchuk*[,‡]

Laboratoire de Chimie du Solide et Inorganique Moléculaire, UMR 6511 CNRS-Université de Rennes 1, Institut de Chimie de Rennes, Avenue du Général Leclerc, 35042 Rennes Cedex, France, and L.V. Pisarzhevskii Institute of Physical Chemistry of the National Academy of Sciences of the Ukraine, prospekt Nauki 31, 03039 Kiev, Ukraine

Received April 8, 2005

Three new homo- and heterometallic hexanuclear complexes $[Mn_2M^{II}_4O_2(PhCOO)_{10}(DMF)_4]$ (with M = Mn (**1**), Co (**2**) or Ni (**3**) and DMF = dimethylformamide) have been synthesized by redox generation of benzoate ligands from benzaldehyde in a one-pot reaction. All of the compounds are isostructural and crystallize in the *I*-42*d* space group of the tetragonal system, data for **1**: $a = 27.2249(8)$ Å, $c = 25.5182(5)$ Å, R1 = 0.0681. The crystal structure contains isolated molecules. Each molecule consists of 2 × Mn^{III} surrounded by four M^{II} ions to form two edge-sharing OMn_2M_2 tetrahedra giving rise to the $[Mn_2M_4O_2]$ core. The coordination sphere of each metal is completed by the bridging benzoate ligands and DMF molecules. The magnetic susceptibilities of **1**–**3** have been measured in the 1.8 K < *T* < 300 K temperature range. The magnetic susceptibilities for **1** and **2** pass through a broad maximum at low temperature which is characteristic of the diamagnetic ground state, while for **3** no maximum is detected down to 1.8 K. The magnetic data have been interpreted quantitatively for **1** and **3** on the basis of spin exchange interactions between the metallic centers (spin Hamiltonian for a pair being $H_{AB} = -\mathbf{J_{AB}}\ \mathbf{S_A}\cdot\mathbf{S_B}$). Single-crystal measurements on $[Mn_6O_2(PhCOO)_{10}(CH_3CN)_4]$ (**4**) show that significant magnetic anisotropy develops at low temperature.

Introduction

3d metal polynuclear oxocarboxylate complexes are currently widely investigated mainly because of their interesting magnetic properties.[1] Actually, many of these compounds possess a large number of unpaired electrons and therefore intramolecular spin−spin interactions. In such systems, along with appreciable magnetic anisotropy, this can lead to a high magnetization relaxation barrier in single molecules. Complexes with these properties are called single-molecule magnets (SMMs). Although complexes of some 3d metals display SMM properties (vanadium,[2] iron,[3] cobalt,[4] and nickel[5]), the majority of SMMs have been found among manganese(III) polynuclear carboxylates.[1] Besides, Mn carboxylate clusters can be used as models of active sites of some enzymes[6a−c] and photosystem II.[6d] The activity in the field of polynuclear systems was mainly focused on the study of homometallic complexes, whereas the investigation of their heteropolynuclear analogues was rather scarce because of difficulties encountered in the synthesis of such com-

* To whom correspondence should be addressed. E-mail: lahcene.ouahab@univ-rennes1.fr; shchuk@inphyschem-nas.kiev.ua.

† Laboratoire de Chimie du Solide et Inorganique Moléculaire, CNRS-Université de Rennes 1.

‡ L.V. Pisarzhevskii Institute of Physical Chemistry of the National Academy of Sciences of the Ukraine.

(1) (a) Gatteschi, D.; Sessoli, R. *Angew. Chem., Int. Ed.* **2003**, *42*, 268 and references therein. (b) Price, J. P.; Batten, S. R.; Moubaraki, B.; Murray, K. S. *Chem. Commun.* **2002**, 762. (c) Brechin, E. K.; Boskovic, C.; Wernsdorfer, W.; Yoo, J.; Yamaguchi, A.; Sañudo, E. C.; Concolino, T. R.; Rheingold, A. L.; Ishimoto, H.; Hendrickson, D. N.; Christou, G. *J. Am. Chem. Soc.* **2002**, *124*, 9710. (d) Jones, L. F.; Brechin, E. K.; Collison, D.; Harrison, A.; Teat, S. J.; Wernsdorfer, W. *Chem. Commun.* **2002**, 2974. (e) Soler, M.; Rumberger, E.; Folting, K.; Hendrickson, D. N.; Christou, G. *Polyhedron* **2001**, *20*, 1365. (f) Soler, M.; Wernsdorfer, W.; Folting, K.; Pink, M.; Christou, G. *J. Am. Chem. Soc.* **2004**, *126*, 2156. (g) Saòudo, E. C.; Wernsdorfer, W.; Abboud, K. A.; Christou, G. *Inorg. Chem.* **2004**, *43*, 4137. (h) Chakov, N. E.; Wernsdorfer, W.; Abboud, K. A.; Christou, G. *Inorg. Chem.* **2004**, *43*, 5919. (i) Milios, C. J.; Raptopoulou, C. P.; Terzis, A.; Lloret, F.; Vicente, R.; Perlepes, S. P.; Escuer, A. *Angew. Chem., Int. Ed.* **2004**, *43*, 210. (j) Coronado, E.; Forment-Aliaga, A.; Gaita-Ariño, A.; Giménez-Saiz, C.; Romero, F. M.; Wernsdorfer, W. *Angew. Chem., Int. Ed.* **2004**, *45*, 6152.

(2) Sun, Z.; Grant, C. M.; Castro, S. L.; Hendrickson, D. N.; Christou, G. *Chem. Commun*. **1998**, 721.

10.1021/ic0505448 CCC: $30.25
Published on Web 07/02/2005

pounds. One can expect that heterometallic complexes may display different physical and chemical properties in comparison with homometallic compounds. For example, substitution of one chromium ion in $[Cr_8F_8(piv)_{16}]$ (where pivH is pivalic acid) for Ni^{II}, Mn^{II}, Fe^{II}, or Cd^{II} ion increased the spin of the ground state of the resulting heterometallic compounds.[7] Therefore, the development of new and efficient synthetic methods for the preparation of 3d metal complexes with a different type of transition metal ions is still an actual challenge.

The most widely characterized and investigated class of SMMs is Mn_{12} clusters containing simultaneously, inside the same coordination skeleton, both Mn^{III} and Mn^{IV} ions. Another well-characterized mixed-valence manganese skeleton is $[Mn_6O_2]^{n+}$ (where $n = 10$ or 14).[8] Among complexes of this type, only the $[Mn^{III}_6O_2(CH_3COO)_2(salox)_6(C_2H_5OH)_4]$ ($saloxH_2$ = salicylaldoxime) complex containing solely Mn^{III} cations revealed SMM properties.[1i] In contrast, in complexes of the $[Mn^{III}_2Mn^{II}_4O_2]^{10+}$ type, interactions between metal ions are antiferromagnetic, giving rise to a diamagnetic ground state. It is therefore interesting to replace Mn^{II} ions in this core by other divalent metals ions to investigate the influence of such substitution on the magnetic properties.

In this work, we report the synthesis, structure, and magnetic properties of three new homo- and heterometallic complexes, namely, $[Mn^{III}_2M^{II}_4O_2(PhCOO)_{10}(DMF)_4]$ (with M = Mn (**1**), Co (**2**), or Ni (**3**) and DMF = dimethylformamide), which were synthesized by a novel strategy based on a so-called in situ ligand redox generation.[9] The single-crystal magnetic measurements of $[Mn^{III}_2Mn^{II}_4O_2(PhCOO)_{10}(CH_3CN)_4]$ (**4**) are also presented.

Experimental Section

Synthesis. Commercially available reagents and solvents were used without further purification.

$[Mn_6O_2(PhCOO)_{10}(DMF)_4]$ (1). $Mn(NO_3)_2\cdot 6H_2O$ (574 mg, 2.00 mmol) was added to benzaldehyde (5 mL), and the mixture was boiled for 5 min with periodic stirring; NO_2 was released from the reaction mixture as brown vapor during this procedure. A mixture of toluene (5 mL) and dimethylformamide (0.5 mL) was added, and the solution was warmed again to the boiling point and then cooled to room temperature. Ether diffusion resulted in the formation of brown crystals within several days. The crystals were filtered off, washed with toluene, and dried under vacuum during several hours. Yield is 405 mg (66.4%). Anal. Calcd for **1** (Found): C, 52.80 (52.61); H, 4.21 (4.26); N, 3.00 (3.01); Mn, 17.67 (17.58).

$[Mn_2Co_4O_2(PhCOO)_{10}(DMF)_4]$ (2). This compound was prepared following the same procedure as for compound **1** using a solution of $Co(NO_3)_2\cdot 6H_2O$ (291 mg, 1.00 mmol) and $Mn(NO_3)_2\cdot 6H_2O$ (144 mg, 0.50 mmol) in a few drops of water. Red-brown crystals were filtered off, washed with toluene, and dried under vacuum during several hours. Yield is 215 mg (46.5%). Anal. Calcd for **2** (Found): C, 52.35 (52.21); H, 4.18 (4.24); N, 2.97 (3.03); Mn, 5.84 (5.75); Co, 12.53 (12.45).

$[Mn_2Ni_4O_2(PhCOO)_{10}(DMF)_4]$ (3). This compound was prepared following the similar procedure described for compound **2** using $Ni(NO_3)_2\cdot 6H_2O$ (582 mg, 2.00 mmol) and $Mn(NO_3)_2\cdot 6H_2O$ (144 mg, 0.50 mmol). Yield is 290 mg (54.6%). Anal. Calcd for **3** (Found): C, 52.38 (52.30); H, 4.18 (4.24); N, 2.98 (3.11); Mn, 5.84 (5.80); Ni, 12.49 (12.55).

$[Mn_6O_2(PhCOO)_{10}(MeCN)_4]$ (4). $Mn(NO_3)_2\cdot 6H_2O$ (500 mg, 1.74 mmol) was dissolved in a few drops of water, then 3 mL of benzaldehyde was added to this solution. The reaction mixture was boiled with periodic stirring for 10 min and then cooled to room temperature and layered with 10 mL of acetonitrile. After several days, the resulting dark red-brown crystals were collected by filtration, washed with acetonitrile, and dried in air for a short time. Yield is 365 mg (72.5%). Anal. Calcd for **4** (Found): C, 53.94 (54.11); H, 3.60 (3.54); N, 3.22 (3.12); Mn, 18.98 (19.07).

Crystallographic Data Collection and Structure Determination. Single crystals of the title compounds were mounted on a Nonius four circle diffractometer equipped with a CCD camera and a graphite monochromated Mo Kα radiation source ($\lambda = 0.71073$ Å) from the Centre de Diffractométrie (CDFIX), Université de Rennes 1, France. Since the structure of compound **4** has been reported previously,[8i] data were collected only for complexes **1**−**3**.

(3) (a) Gatteschi, D.; Sessoli, R.; Cornia, A. *Chem. Commun.* **2000**, 725. (b) Delfs, C.; Gatteschi, D.; Pardi, L.; Sessoli, R.; Wieghardt, K.; Hanke, D. *Inorg. Chem.* **1993**, *32*, 3099. (c) Benelli, C.; Cano, J.; Journaux, Y.; Sessoli, R.; Solan, G. A.; Winpenny, R. E. P. *Inorg. Chem.* **2001**, *40*, 188. (d) Goodwin, J. C.; Sessoli, R.; Gatteschi, D.; Wernsdorfer, W.; Powell, A. K.; Heath, S. L. *J. Chem. Soc., Dalton Trans.* **2000**, 1835.

(4) Yang, E.-C.; Hendrickson, D. N.; Wernsdorfer, W.; Nakano, M.; Zakharo, L. N.; Sommer, R. D.; Rheingold, A. L.; Ledezma-Gairaud, M.; Christou, G. *J. Appl. Phys.* **2002**, *91*, 7382.

(5) (a) Nakano, M.; Matsubayashi, G.-E.; Takaki, M.; Tatsuo, C. K.; Amaya, K.; Yoo, J.; Christou, G.; Hendrickson, D. N. *Mol. Cryst. Liq. Cryst. Sci. Technol., Sect. A* **2002**, *376*, 405. (b) Boskovic, C.; Rusanov, E.; Stoeckli-Evans, H.; Güdel, H. U. *Inorg. Chem. Commun.* **2002**, *5*, 881. (c) Cadiou, C.; Murrie, M.; Paulsen, C.; Villar, V.; Wernsdorfer, W.; Winpenny, R. E. P. *Chem. Commun.* **2001**, 2666. (d) Andres, H.; Basler, R.; Blake, A. J.; Cadiou, C.; Chaboussant, G.; Grant, C. M.; Güdel, H.-U.; Murrie, M.; Simons, S.; Paulsen, C.; Semadini, F.; Villar, V.; Wernsdorfer, W.; Winpenny, R. E. P. *Chem. −Eur. J.* **2002**, *8*, 4867. (e) Ochsenbein, S. T.; Murrie, M.; Rusanov, E.; Stoeckli-Evans, H.; Sekine, C.; Güdel, H. U. *Inorg. Chem.* **2002**, *41*, 5133.

(6) (a) Wu, A. J.; Penner-Hahn, J. E.; Pecoraro, V. L. *Chem. Rev.* **2004**, *104*, 903 and references therein. (b) Wu, J.-Z.; Sellitto, E.; Yap, G. P. A.; Sheats, J.; Dismukes, G. C. *Inorg. Chem.* **2004**, *43*, 5795. (c) Ferreira, K. N.; Iverson, T. M.; Maghlaoui, K.; Barber, J.; Iwata, S. *Science* **2004**, *303*, 1831. (d) Mukhopadhyay, S.; Mandal, S. K.; Bhaduri, S.; Armstrong, W. H. *Chem. Rev.* **2004**, *104*, 3981 and references therein.

(7) (a) van Slageren, J.; Sessoli, R.; Gatteschi, D.; Smith, A. A.; Helliwell, M.; Winpenny, R. E. P.; Cornia, A.; Barra, L.-A.; Jansen, A. G. M.; Timco, G. A.; Rentschler, E. *Chem. −Eur. J.* **2002**, *8*, 277. (b) Larsen, F. K.; McInnes, E. J. L.; El Mkami, H.; Overgaard, J.; Piligkos, S.; Rajaraman, G.; Rentschler, E.; Smith, A. A.; Smith, G. M.; Boote, V.; Jennings, M.; Timco, G. A.; Winpenny, R. E. P. *Angew. Chem., Int. Ed.* **2003**, *42*, 101. (c) Gavrilenko, K. S.; Vértes, A.; Vanko, G.; Kiss, L. F.; Addison, A. W.; Weyhermüller, T.; Pavlishchuk, V. V. *Eur. J. Inorg. Chem.* **2002**, 3347.

(8) (a) Kim, J.; Cho, H. *Inorg. Chem. Commun.* **2004**, *7*, 122. (b) Murrie, M.; Parsons, S.; Winpenny, R. E. P. *J. Chem. Soc., Dalton Trans.* **1998**, 1423. (c) Plackman, A. G.; Huffman, J. C.; Lobkovsky, E. B.; Christou, G. *Polyhedron* **1992**, *11*, 251. (d) Karsten, P.; Strahle, J. *Acta Crystallogr. C* **1998**, *54*, 1403. (e) Baikie, A. R. E.; Howes, A. J.; Hursthouse, M. B.; Quick, Q. B.; Thornton, P. *J. Chem. Soc., Chem. Commun.* **1986**, 1587. (f) Kohler, K.; Roesky, H. W.; Noltemeyer, M.; Schmidt, H.-G.; Freire-Erdbrügger, C.; Sheldrick, G. M. *Chem. Ber.* **1993**, *126*, 921. (g) Schake, A. R.; Vincent, J. B.; Li, Q.; Boyd, P. D. W.; Folting, K.; Huffman, J. C.; Hendrickson, D. N.; Christou, G. *Inorg. Chem.* **1989**, *28*, 1915. (h) Batsanov, A. S.; Struchkov, Y. T.; Timko, G. A.; Gerbeleu, N. V.; Manole, O. S.; Grebenko, S. V. *Russ. J. Coord. Chem.* **1994**, *20*, 604. (i) Halcrow, M. A.; Streib, W. E.; Folting, K.; Christou, G. *Acta Crystallogr. C* **1995**, *51*, 1263.

(9) Gavrilenko, S. K.; Punin, S. V.; Cador, O.; Golhen, S.; Ouahab, L.; Pavlishchuk, V. V. Unpublished work.

Table 1. Crystal Data and Structure Refinement for **1**, **2**, and **3**

	1	**2**	**3**
empirical formula	$Mn_6C_{82}H_{78}N_4O_{26}$	$Mn_2Co_4C_{82}H_{78}N_4O_{26}$	$Mn_2Ni_4C_{82}H_{78}N_4O_{26}$
formula weight/ g·mol^{-1}	1865.12	1881.08	1880.20
temperature/K	293 (2)	293 (2)	293 (2)
wavelength/Å	0.71073	0.71073	0.71073
crystal system	tetragonal	tetragonal	tetragonal
space group	*I*-42*d*	*I*-42*d*	*I*-42*d*
a/Å	27.2249 (8)	27.1017 (9)	27.0152 (9)
c/Å	25.5182 (5)	25.3740 (4)	25.2913 (5)
volume/Å^3	18914.0 (9)	18637.3 (9)	18458.1 (9)
Z	8	8	8
calcd density/g·cm^{-3}	1.310	1.341	1.353
absorption coefficient/mm^{-1}	0.847	1.030	1.137
F(000)	7648	7712	7744
θ range for data collection/deg	2.12−25.30	5.00−25.35	5.02−26.02
reflctns collected	31676	15648	16679
reflctns unique	8107	8129	8731
R(int)	0.1281	0.0345	0.0392
parameters	533	533	533
goodness-of-fit on F^2	1.231	1.077	1.048
$R_1{}^a$ [$I > 2\sigma(I)$]	0.0681	0.0495	0.0517
wR2^b [$I > 2\sigma(I)$]	0.1523	0.1296	0.1296

^{a} $R_1 = \sum||F_o| - |F_c||/\sum|F_o|$. ^{b} wR2 = $\{\sum[w(F_o^2 - F_c^2)^2]/\sum[w(F_o^2)^2]\}^{1/2}$.

Table 2. Selected Distances (Å) for **1**−**3**

1			**2**	**3**
Mn1−Mn2	2.810(3)		2.812(2)	2.807(2)
Mn1−O13	1.886(6)		1.889(4)	1.895(4)
Mn1−O10	1.944(6)		1.939(4)	1.936(4)
Mn1−O1	2.288(5)		2.248(3)	2.236(3)
Mn2−O13	1.897(6)		1.898(4)	1.894(4)
Mn2−O4	1.924(7)		1.946(4)	1.950(4)
Mn2−O5	2.218(5)		2.211(4)	2.200(4)
Mn3−O2	2.150(6)	M1−O2	2.089(4)	2.060(4)
Mn3−O8	2.086(6)	M1−O8	2.036(4)	2.003(4)
Mn3−O3	2.175(7)	M1−O3	2.106(5)	2.058(5)
Mn3−O11	2.176(6)	M1−O11	2.110(4)	2.079(4)
Mn3−O13	2.194(6)	M1−O13	2.115(4)	2.074(4)
Mn3−O5	2.331(6)	M1−O5	2.236(4)	2.175(4)
Mn4−O7	2.143(7)	M2−O7	2.072(4)	2.042(4)
Mn4−O6	2.105(7)	M2−O6	2.046(5)	2.024(5)
Mn4−O9	2.178(7)	M2−O9	2.071(5)	2.030(5)
Mn4−O12	2.189(7)	M2−O12	2.119(5)	2.069(4)
Mn4−O13	2.204(5)	M2−O13	2.102(3)	2.071(3)
Mn4−O1	2.308(7)	M2−O1	2.237(4)	2.183(4)

Effective absorption correction was performed (SCALEPACK[10]). The structure of **1** was solved with the direct method using Sir-97; the structures of **1** and isostructural compounds **2** and **3** were refined with the full-matrix least-squares method on F^2 using the SHELXL-97 program. Crystallographic data are summarized in Table 1; selected bond lengths are given in Table 2. Complete crystal structure results as CIF files, including bond lengths, bond angles, and atomic coordinates, are deposited as Supporting Information.

Magnetic Measurements. The magnetization have been recorded with a Quantum Design MPMS SQUID magnetometer operating in the temperature range of 2−300 K with a dc magnetic field up to 5 T. χ_M stands for the molar magnetic susceptibility and *T* the temperature in Kelvin. The experimental data have been corrected from the diamagnetism of the sample holder, and the intrinsic diamagnetism of the materials has been evaluated with Pascal's tables.

Results and Discussion

Synthesis. Several approaches leading to the isolation of manganese hexanuclear oxocarboxylate complexes with a $[Mn_6O_2]^{10+}$ core are known.[8] These methods can be divided into two groups: the first one is based on Mn^{II} carboxylates oxidation with oxygen,[8b,d,e,h] potassium permanganate,[8c] or di-(trimethylsilyl)peroxide.[8f] The second route includes reduction with the subsequent coupling of trinuclear $[Mn_3O]^{6+}$ moieties resulting in $[Mn_6O_2]^{10+}$ formation. Reducing agents either sodium acenaphthylenide[8g] or toluene[8a] which are oxidized to benzyl alcohol were used. Finally, the $[Mn_6O_2^{10+}]$ unit was constructed by reduction of the tetranuclear $[Mn_4O_2]^{8+}$ core.[8i] In all of the above-mentioned cases, the carboxylate ions were already present in the coordination core or in the reaction mixture and were not involved in any redox process. Heterometallic complexes with a similar $[Mn^{III}_2M^{II}_4O_2]^{10+}$ polynuclear moiety are unknown so far.

In this paper, we provide an easy one-pot redox reaction for the synthesis of a $[Mn_2M^{II}_4O_2]^{10+}$ (M = Mn, Co and Ni) core. The interaction of metal nitrates with benzaldehyde under aerobic conditions results in direct in situ generation of both Mn^{III} ions and benzoate anions in one step by an oxidation process of Mn^{II} and benzaldehyde with nitrate. These redox processes can be described by the following equations

$$4PhCHO + 4NO_3^- + O_2 = 4PhCOO^- + 4NO_2\uparrow + 2H_2O\uparrow \quad (1)$$

$$4PhCHO + 4Mn^{2+} + 3O_2 = 4PhCOO^- + 4Mn^{3+} + 2H_2O\uparrow \quad (2)$$

As the main product isolated from the reaction mixture reveals $[Mn^{III}_2Mn^{II}_4O_2]^{10+}$ composition and contains simultaneously Mn^{II} and Mn^{III} inside this moiety, one can assume that Mn^{II} is partially oxidized to Mn^{III} according to **2**. Also, the excess of benzaldehyde present in the reaction mixture reduces some amount of Mn^{III}

$$2Mn^{3+} + PhCHO + H_2O = 2Mn^{2+} + PhCOOH + 2H^+ \quad (3)$$

(10) Otwinowski, Z.; Minor, W. Processing of X-ray Diffraction Data Collected in Oscillation Mode. *Macromolecular Crystallography. Part A*; Carter, C.W., Jr., Sweet, R. M., Eds.; Methods in Enzymology, Academic Press: 1997; Vol. 276, pp 307−326.

This process is accompanied by color changes from colorless to dark brown and light brown at the end of the redox processes. The deep brown color can be attributed to the formation of Mn^{III} oxocarboxylate species after Mn^{II} oxidation at the beginning of the process (eq 2). Finally, the solution lightening can be attributed to partial reduction of Mn^{III} species by an excess of benzaldehyde (eq 3).

After the addition of the toluene−DMF mixture to the reaction pot, the mixed-valence manganese complex $[Mn_6O_2(PhCOO)_{10}(DMF)_4]$ (**1**) was isolated. The overall process can be described by the following equation

$$4Mn^{2+} + 2Mn^{3+} + 2H_2O + 14PhCOO^- + 4DMF = [Mn_6O_2(PhCOO)_{10}(DMF)_4] + 4PhCOOH \quad (4)$$

Consequently, the formation of **1** can be described

$$12Mn(NO_3)_2 + 20PhCHO + 5O_2 + 8DMF = 2[Mn_6O_2(PhCOO)_{10}(DMF)_4] + 24NO_2\uparrow + 10H_2O \quad (5)$$

It is evident that processes which lead to the formation of the above-mentioned polynuclear moieties are more intricate than those presented by foregoing reactions. There is no doubt that the formation of $[Mn_6O_2(PhCOO)_{10}(L)_4]$ moieties under the reaction conditions is a delicate balance between major factors such as (i) thermodynamic stability of $[Mn_6O_2]^{10+}$ skeleton and (ii) crystal lattice energies for $[Mn_6O_2(PhCOO)_{10}(L)_4]$ complexes.

It is worthy to notice that this method allows the synthesis of the known complex **4** with better yield.[8] Complex **4** is not stable as it loses acetonitrile molecules. Recrystallization of **4** from a toluene−DMF mixture also yields the stable complex $[Mn_6O_2(PhCOO)_{10}(DMF)_4]$ (**1**).

This method was extended to the synthesis of the heterometallic derivatives containing different M^{II} such as Co^{II} or Ni^{II} instead of Mn^{II}. For example, starting from a stoichiometric mixture (2:1) of cobalt and manganese nitrates we obtained compound **2** following the equation

$$4Mn(NO_3)_2 + 8Co(NO_3)_2 + 20PhCHO + 5O_2 + 8DMF = 2[Mn_2Co_4O_2(PhCOO)_{10}(DMF)_4] + 24NO_2\uparrow + 10H_2O\uparrow \quad (6)$$

However, complex **3** was obtained by using an excess of nickel nitrate in the 1:4 Mn-to-Ni ratio; all of the attempts to synthesize complex **3** using stoichiometric amounts of metal nitrates gave only compounds with an intermediate Mn/Ni ratio between 1 and 2.

Crystal Structures. Compounds **1**−**3** are isostructural. Their molecular structures are reminiscent to that of the tetramanganese(II) dimanganese(III) compound **4** reported previously,[8i] although they crystallize in different crystal systems and they have differently coordinated solvent molecules.

Compound 1. The molecular structure of complex (**1**) is shown in Figure 1. The asymmetric unit contains four nonequivalent manganese ions, giving rise to six manganese ions arranged as two edge-shared distorted tetrahedra. The μ_4-$O10^{2-}$ ion is located at the center of each tetrahedron. Peripheral ligation consists of 10 bridging benzoate ions and 4 terminal DMF molecules; some benzoate ions are coordinating in $\mu_2(\eta_1,\eta_2)$ mode whereas the remaining ligands present a $\mu_3(\eta_1,\eta_2)$ coordination mode. Manganese ions present a distorted octahedron coordination sphere. Bond lengths (Table 2) and charge considerations suggest a mixed-valence $Mn^{III}Mn^{II}$ nature for this complex. Mn^{III} ions defined the shared edge of tetrahedra (Mn1 and Mn2). The equatorial Mn(1, 2)−O(13, 10, 4) distances (1.886(6)−1.944(6) Å) are shorter than those corresponding to the Mn(3, 4)−O(2, 3, 6−9, 11, 12) (2.086(6)−2.331(6) Å). The axial bond lengths Mn1−O1 and Mn2−O5 are equal to 2.288(5) and 2.218(5) Å, respectively. Thus, Mn1 and Mn2 ions present a strong Jahn−Teller elongation, which confirms the 3+ oxidation states for both of them. The shortest Mn−Mn distance is equal to 2.810(3) Å (Mn1−Mn2).

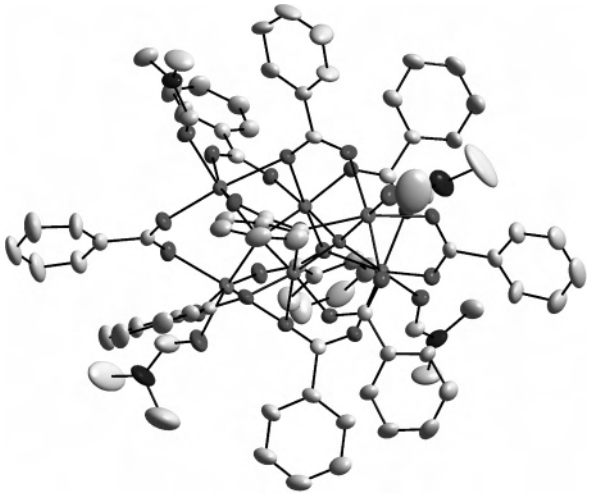

Figure 1. Structure of complex **1** with 30% probability level.

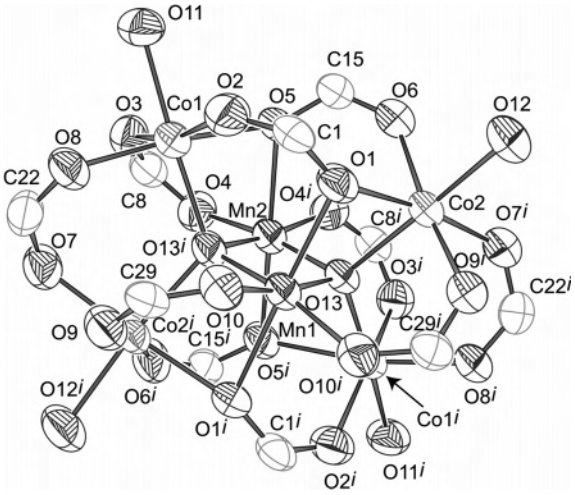

Figure 2. ORTEP drawing of complex **2** with 50% probability level, aromatic rings were omitted for clarity. Symmetry *i*: x, $^1/_2 - y$, $^1/_4 - z$.

Compounds 2 and 3. Structural details of **2** are presented, and the corresponding data for **3** are given in brackets. The molecular structure of **2** with the atomic numbering scheme is shown in Figure 2, and selected bond distances for **2**) and **3** are given in Table 2. The molecular structures of **2** and **3** are similar, and hence, we give here only an ORTEP drawing for **2**. The labeling scheme is the same for both compounds with Co1 [Ni1] and Co2 [Ni2] replacing Mn3 and Mn4,

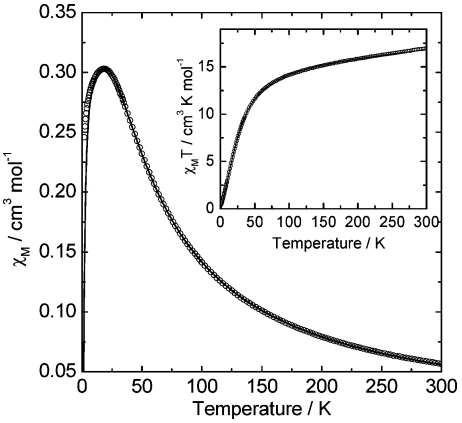

Figure 3. Temperature dependence χ_M of **1**: empty circles, experimental points; full line, best agreement with theory (see text). Inset, temperature dependence of $\chi_M T$.

respectively. The asymmetric unit contains four metallic sites as two Mn^{III} and two M^{II} in general positions. This yields a core containing six octahedrally coordinated metal centers with two Mn^{III} and four M^{II} ions. The metal atoms form two M^{II}_2−Mn^{III}_2 tetrahedra sharing their Mn^{III}−Mn^{III} edge (see Figure 3). The μ_4-O10 atom is located at the center of each tetrahedron giving rise to a $[Mn^{III}_2M^{II}_4O_2]$ unit.

The molecular structure of these complexes is similar to **1** with distorted octahedral geometry around Mn^{III} ions. O−Mn−O′ angles (where O and O′ are neighboring atoms) are ranging from 83.9(2) to 98.4(2)° [83.9(2) to 98.5(2)°]. The Mn^{III}−O distances can be separated into two groups: four equatorial Mn−O10 and Mn−O13 (1.889(3)−1.939(4) Å) [1.895(4)−1.936(4) Å] and two axial Mn1−O1 (2.248(3) [2.236(3)] Å). These distances are similar to those observed in complex **1** (Table 2). Mn^{III} ions exhibit a Jahn−Teller distortion along the O1−Mn−O1* axis. The Mn1−Mn2 distance is equal to 2.812(2) [2.807(2)] Å.

In both complexes **2** and **3**, the M^{II} ions have a distorted octahedral $[M^{II}O_6]$ geometry. Each M^{II} cation is coordinated to four oxygen atoms from four bridging benzoate ligands, the two remaining positions being occupied by the oxygen atom of the DMF molecule (O11 for M1 and O12 for M2) and the μ_4-O13 atom. Two benzoate ions act as μ_2-bridges between the M^{II} metallic site via O7 and O8 atoms; four others are μ_2-bridging one M^{II} and one Mn via O3, O4 and O9, O10. Each of the four last benzoate ligands is connecting three metallic ions in the $\mu_3(\eta_1,\eta_2)$ mode. The η_2-O atom of μ_3-benzoate is coordinated to the M^{II} and Mn^{III} ions and the η_1-O to the other divalent metal ions. The longest M^{II}−O bonds in each $[M^{II}O_6]$ octahedron take place between the metal and η_2-O atoms from the $\mu_3(\eta_2,\eta_1)$-benzoate bridges: Co1−O5 (2.236(4) [2.175(4)] Å) and Co2−O1 (2.237(4) [2.183(4)] Å). The shortest distances (from 2.036(4) [2.003(4)] to 2.106(4) [2.060(4)] Å) are observed between metal ions and other oxygen atoms from the μ-benzoates (O2, O3, O8 for M1 and O6, O7, O9 for M2, see Table 2). The four average bond lengths Co1−μ_4-O13 (2.115(4) [2.070(3)] Å), Co2−μ_4-O13 (2.102(3) [2.074(4)] Å), Co1−O11(DMF) (2.110(4) [2.079(4)] Å), and Co2−O12(DMF) (2.119(4) [2.069(4)] Å) are observed. The Co−O [Ni−O] bond lengths are similar to those observed in other polynuclear complexes.[5,11,12]

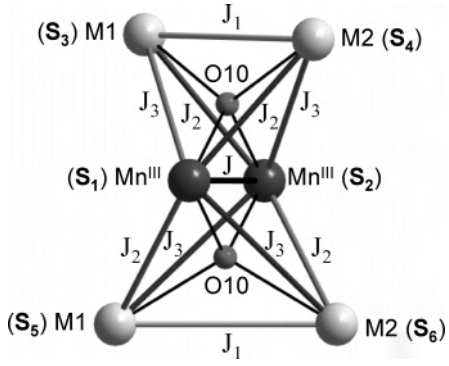

Figure 4. Scheme representing the two $[Mn^{III}_2M^{II}_2O]$ tetrahedra with exchange pathways between the local spins.

Analytical data of complexes **2** and **3** are in good agreement with the Mn/M^{II} 1:2 ratio. In addition, from the crystallographic data (Table 2), the Jahn−Teller distortion of two metallic sites allows us to attribute these positions to Mn^{III} ions while the remaining sites are occupied by M^{II} ions. Moreover, M^{II}−O bond lengths in **2** and **3** are shorter than the analogous distances in **1** (Table 2) because the ionic radii of Co^{II} (0.885 Å) and Ni^{II} (0.83 Å) are smaller than that of Mn^{II} (0.97 Å).[14]

Magnetic Properties. The temperature dependencies of molar magnetic susceptibility (χ_M) and $\chi_M T$ for **1** are represented in Figure 3. At room temperature, $\chi_M T$ is equal to 16.97 cm^3 K mol^{-1}, which is much below the expected spin-only value for six isolated magnetic centers (4 × Mn^{II} with $S_{Mn} = {}^5/_2$ and 2 × Mn^{III} with $S_{Mn} = 2$) considering an average Zeeman factor $g = 2.00$, that is, 23.5 cm^3 K mol^{-1}. This observation is in agreement with the room temperature $\chi_M T$ values published for other $[Mn^{III}_2Mn^{II}_4O_2]^{10+}$ clusters with identical core structures.[8a,8g,13] When the temperature is lowered, χ_M increases and passes through a rounded maximum at $T_{max} = 20$ K. This indicates that antiferromagnetic interactions operate between 3d magnetic centers within the cluster. We represent in Figure 4 the coupling scheme between the magnetic centers in cluster **1** with the two edge-sharing $[OMn_4]$ tetrahedra.

The Heisenberg spin Hamiltonian describing the system is the following

$$H = -J\,\vec{S}_1\cdot\vec{S}_2 - J_1(\vec{S}_3\cdot\vec{S}_4 + \vec{S}_5\cdot\vec{S}_6) - J_2(\vec{S}_2\cdot\vec{S}_3 + \vec{S}_1\cdot\vec{S}_4 + \vec{S}_1\cdot\vec{S}_5 + \vec{S}_2\cdot\vec{S}_6) - J_3(\vec{S}_1\cdot\vec{S}_3 + \vec{S}_2\cdot\vec{S}_4 + \vec{S}_1\cdot\vec{S}_6 + \vec{S}_2\cdot\vec{S}_5) \quad (7)$$

(11) Aromí, G.; Batsanov, A. S.; Christian, P.; Helliwell, M.; Parkin, A.; Parsons, S.; Smith, A. A.; Timco, G. A.; Winpenny, R. E. P. *Chem. −Eur. J.* **2003**, *9*, 5142.
(12) Cadiou, C.; Coxall, R. A.; Graham, A.; Harrison, A.; Helliwell, M.; Parsons, R.; Winpenny, R. E. P. *Chem Commun.* **2002**, 1106. (b) Eremenko, I. L.; Malkov, A. E.; Sidorov, A. A.; Fomina, I. G.; Aleksandrov, G. G.; Nefedov, S. E.; Rusinov, G. L.; Chupakhin, O. N.; Novotortsev, V. M.; Ikorskii, V. N.; Moiseev, I. I. *Inorg. Chim. Acta* **2002**, *334*, 334.
(13) Baikie, A. R. E.; Howes, A. J.; Hursthouse, M. B.; Quick, A. B.; Thornton, P. *J. Chem. Soc., Chem. Commun.* **1986**, 187.
(14) Shannon, R. D. *Acta Crystallogr., Sect. A* **1976**, *32*, 751.

The spin Hamiltonian consists of only the terms for which the exchange pathways could circulate through the μ_4-O^{2-} ions. It is mathematically possible to fit the experimental curve with programs that calculate the magnetic susceptibility on the basis of eq 7 and the Van Vleck equation.[15] However, the exact fit of experimental data was achieved only after including an average Zeeman factor with four additional parameters, thus the model became overparametrized and with a strong dependency among them. J_2 and J_3 were considered as equal in order to simplify the model (see Figure 4). Actually, this is not true because of the different pathways for these interactions: two carboxylate groups and μ_4-O^{2-} for J_2 and only one carboxylate group and μ_4-O^{2-} for J_3.

The resulting model consists of four parameters, namely, g, J, J_1, and J_2. The best agreement between the experimental data and calculated curve was found using the minimization package CLUMIN[16] in the temperature range 10−300 K. The best calculated curve is represented in Figure 3 with $g = 1.99$, $J = -101$ cm^{-1}, $J_1 = -4.23$ cm^{-1}, and $J_2 = J_3 = -8.32$ cm^{-1} in excellent agreement with the experimental value. This set of parameters agrees with the previous analysis of a similar metallic core cluster except for J_2, which is found at a slightly higher value.[8g] One must notice that J and J_2 are correlated. Indeed, good agreement between theory and experiment is found in fixing $J_2 = J_3 = 0$ cm^{-1} and J around -500 cm^{-1}. As long as J dominates in an overwhelming manner over the other superexchange parameters, the system can be considered as two uncoupled Mn^{II} dimers in the low temperature range (below 50 K). The experimental data were fitted with the mathematical expression derived for two uncoupled dimers. The agreement is fairly good with $J_1 = -4.3$ cm^{-1} and $g = 2.01$, values which are close to the ones obtained with the full procedure.

The discrepancy below 10 K may have several origins. First, hexanuclear clusters decompose on air after removal from the mother liquor. The result is the presence of paramagnetic impurities, detectable only at low temperature. Despite our efforts to minimize this problem, we cannot exclude the pollution because of partial decomposition. However, an appropriate term can be added to the equation. Second, single-crystal studies reveal significant magnetic anisotropy at low temperature (see below). If the introduction of appropriate terms reflecting these two possibilities would also overparametrize the model, then we did not attempt to fit the data in the low-temperature range with a full set of parameters.

We performed single-crystal investigations of **4** as its crystals are suitable for such a study.[8i] The core structure is identical, and the powder measurements revealed that the compounds behave in the same manner. The temperature dependence of magnetic susceptibilities measured with the magnetic field (10 000 Oe) applied along the three principal axes is represented in Figure 5. The three susceptibilities pass through a maximum centered at $T_m = 20$, 22, and 22 K for H applied along c, b, and a, respectively. The $H//c$ and $H//a$ curves are almost perfectly superimposed whatever the temperature, while below 20 K the susceptibility along b is bigger. Octahedral Mn^{II} is known to possess small magnetic anisotropy with a zero field splitting (ZFS) parameter D of the order of 0.1 cm^{-1}.[17] Below 50 K, we can neglect the contribution from the Mn^{III}−Mn^{III} moiety. Also, the local ZFS of Mn^{III} (few wavenumbers) is not involved in the global anisotropy of the cluster at low temperature. The Hamiltonian for **1** based on two Mn^{II} dimer models including ZFS of Mn^{II} (D) and Zeeman perturbation (g) reduces to

$$H = -J_1(\vec{S}_3\cdot\vec{S}_4 + \vec{S}_5\cdot\vec{S}_6) + \sum_{i=3,4,5,6}(DS_{i_z}^2 + g\vec{S}_i\cdot\vec{H}) \quad (8)$$

Simulations performed with MAGPACK package[18] show that with $D = -0.2$ cm^{-1}, $J_1 = -4.3$ cm^{-1}, $g = 2.00$, and $H = 10\,000$ Oe, the experimental data can be reproduced. We have supposed an axial-type anisotropy and that the anisotropy axes of Mn^{II} are parallel to b-axis. On Figure 6, we have plotted the experimental and calculated curve of $\Delta\chi_M = \chi_{M\|b} - \chi_{M\perp b}$. The agreement is fairly good except below 3 K, where our model is certainly oversimplified. It

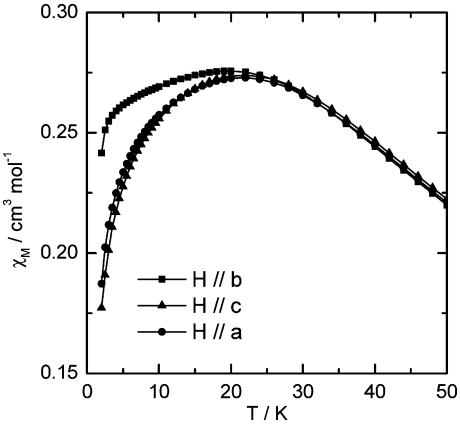

Figure 5. Temperature dependencies of χ_M recorded with the dc external magnetic field H applied along the three crystallographic axes of **4**.

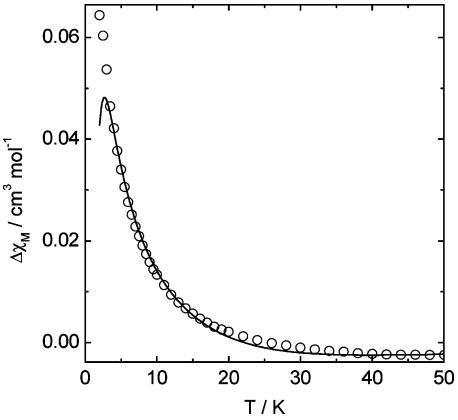

Figure 6. Temperature dependence of $\Delta\chi_M = \chi_{M\|b} - \chi_{M\perp b}$ for **4**: empty circles, experimental points; full line, simulated curve (see text).

(15) Kahn, O. *Molecular Magnetism*; VCH: New York, 1993.
(16) Gatteschi, D.; Pardi, L. *Gazz. Chim. Ital.* **1993**, *123*, 231.
(17) Abragam, A.; Bleaney, B. *Electron Paramagnetic Resonance of Transition Ions*; Dover Publications: New York, 1970.
(18) Borrás-Almenar, J. J.; Clemente-Juan, J. M.; Coronado, E.; Tsukerblat, B. S. *Inorg. Chem.* **1999**, *38*, 6081. Borrás-Almenar, J. J.; Clemente-Juan, J. M.; Coronado, E.; Tsukerblat, B. S. *J. Comput. Chem.* **2001**, *22*, 985.

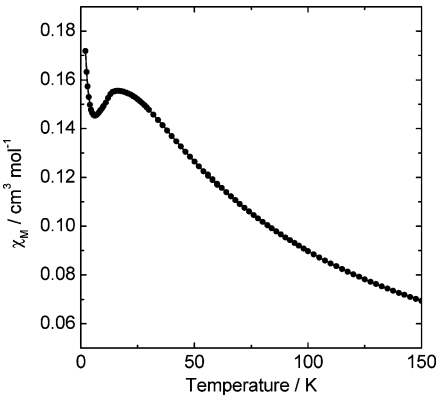

Figure 7. χ_M vs T of a powdered sample of **2**.

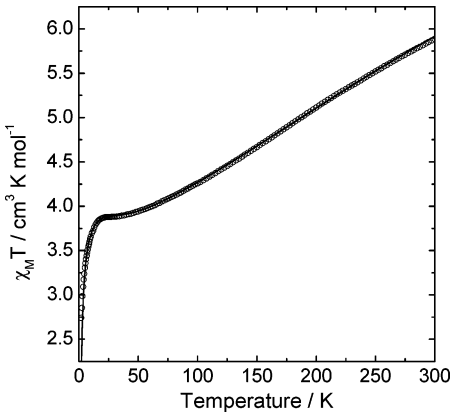

Figure 8. Temperature dependence of $\chi_M T$ of **3**: empty circles, experimental points; full line, best agreement with theory (see text).

is interesting to notice that the positive single ion ZFS gives rise to an apparent negative ZFS at the level of the cluster. This can be simply explained by the fact that when antiferromagnetic isotropic interaction is dominant, the total spin S of a pair of coupled spins is a good quantum number. If we apply this consideration to our system, the effective spin Hamiltonian which describes the magnetic anisotropy for each state S_{34} or S_{56} ($\mathbf{S_{34}} = \mathbf{S_3} + \mathbf{S_4}$ and $\mathbf{S_{56}} = \mathbf{S_5} + \mathbf{S_6}$) within one dimer is

$$H_{S_{34}} = \vec{\boldsymbol{S}}_{34} \cdot \boldsymbol{D}_{S_{34}} \cdot \vec{\boldsymbol{S}}_{34} \tag{9}$$

with D_{34} the anisotropy tensor related to the local anisotropy tensors D_3 and D_4 through coefficients appearing in eq 10

$$\boldsymbol{D}_{S_{34}} = c_{34}\boldsymbol{D}_{S_3} + c'_{34}\boldsymbol{D}_{S_4} \tag{10}$$

tabulated in refs 15 and 19. For the first three thermally populated states, $S_{34} = 1, 2, 3$ the coefficient c_{34} and c_{34}' are negative which transforms planar anisotropy ($D > 0$) into axial anisotropy ($D < 0$).

The χ_M vs T plot of powders of **2** is represented in Figure 7. At room temperature, $\chi_M T$ is equal to 12.57 cm^3 K mol^{-1}. Because of its orbitally degenerated ground state,[15] octahedral Co^{II} does not follow Curie law. The room-temperature value of $\chi_M T$ for isolated octahedral Co^{II} is usually in the range 2.3−3.4 cm^3 K mol^{-1}.[20] The structure of the complex **2** is the same as that in **1**; therefore at room temperature, the contribution from Mn^{III} moiety must be smaller than that for isolated spins. The room-temperature value of $\chi_M T$ supports this hypothesis. When the temperature is lowered, χ_M passes through a broad maximum at $T_{max} = 16$ K which clearly indicates that the ground state of the cluster is diamagnetic with moderate interaction between Co^{II}. The increase at low temperature, below 6 K, is due to the presence of paramagnetic impurities. The extreme sophistication of the magnetic properties of octahedral Co^{II} makes the quantitative analysis of the magnetic properties of **2** complicated, if not impossible.

The temperature dependence of $\chi_M T$ of a powdered sample of **3** is shown in Figure 8. At room temperature, $\chi_M T$ is equal to 5.89 cm^3 K mol^{-1}. This value is below what is expected, that is, 10 cm^3 K mol^{-1}, for isolated spins (four $S_{Ni} = 1.0$ and two $S_{Mn} = 2.0$) with an average Zeeman factor equal to 2.0. When the temperature is lowered, $\chi_M T$ decreases and reaches a plateau below 50 K with $\chi_M T \approx 3.9$ cm^3 K mol^{-1}. This value is very close from the spin-only value obtained for four isolated Ni^{II} spins, that is, 4 cm^3 K mol^{-1}. Finally, $\chi_M T$ drops below ca. 20 K. The fitting of the experimental data in the temperature range 10−300 K with the same model used for **1** (see eq 8) gives $g = 2.02$, $J = -76.9$ cm^{-1}, $J_1 = -1.02$ cm^{-1}, and $J_2 = -11$ cm^{-1} with an excellent agreement between experimental and theoretical values. We did not attempt to fit the data below 10 K because of the presence of Ni^{II} zero field splitting.[17] As expected from structural parameters, the amplitude of the superexchange interaction, J, between the two Mn^{III} ions is almost identical in **1** and **3**.

Conclusion

Three new homo- and hetero-hexanuclear complexes containing a [$Mn^{III}_2M^{II}_4$, M = Mn, Co, Ni] core have been easily synthesized with a good yield and in a short period of time by a novel method based on the in situ generation of benzoate ligands from benzaldehyde. Their crystal structures and magnetic properties have been investigated. The six metal ions arrangement consists of two $Mn^{III}_2M^{II}_2$ tetrahedra sharing their Mn−Mn edge; the center of each tetrahedron is occupied by one oxygen atom bridging four metal ions. The octahedral coordination sphere of each metal is completed by the oxygen atoms from benzoate ligands with different coordination modes and the oxygen atoms from DMF molecules. The magnetic properties of all of the materials reveal that the ground states are nonmagnetic and obviously none of these can be single molecule magnets. The main obstacle in such clusters is that the interaction between the two central Mn^{III} ions is strong and antiferromagnetic. Therefore, at low temperature, the system is equivalent to two uncoupled dimers; the apparent hexanuclearity reduces to binuclearity. Nevertheless, the preparation method affords a heterometallic species in a controlled

(19) Bencini, A.; Gatteschi, D. *EPR of exchange coupled systems*; Springer: Berlin, Germany, 1990.
(20) O'Connor, C. J. *Prog. Inorg. Chem.* **1982**, *29*, 203.

manner. We are now trying to apply our synthetic method to build other bimetallic clusters with high nuclearity and attractive properties.

Acknowledgment. This work was supported by CNRS, INTAS Grant No 03-51-4532. K.S.G. and L.O. thank NATO for postdoctoral fellowship and expert visiting grant to Kiev, respectively.

Supporting Information Available: X-ray crystallographic files in CIF format, for **1**, **2**, and **3**. This material is available free of charge via the Internet at http://pubs.acs.org.

IC0505448